Role of guanylyl cyclase modulation in mouse cone phototransduction

Keisuke Sakurai[1], **Jeannie Chen**[2,3], and **Vladimir J. Kefalov**[1,3]

[1] Department of Ophthalmology and Visual Sciences, Washington University, St. Louis, Saint Louis, MO 63124

[2] Zilkha Neurogenetic Institute, Department of Cell and Neurobiology & Department of Ophthalmology, Keck School of Medicine, University of Southern California, Los Angeles, CA 90033

Abstract

A negative phototransduction feedback in rods and cones is critical for the timely termination of their light responses and for extending their function to a wide range of light intensities. The calcium feedback mechanisms that modulate phototransduction in rods have been studied extensively. However, the corresponding modulation mechanisms that enable cones to terminate rapidly their light responses and to adapt in bright light, properties critical for our daytime vision, are still not understood. In cones, calcium-feedback to guanylyl cyclase is potentially a key step in phototransduction modulation. The guanylyl cyclase activity is modulated by the calcium-binding Guanylyl Cyclase Activating Proteins (GCAP1 and GCAP2). Here, we used single-cell and transretinal recordings from mouse to determine how GCAPs modulate dark-adapted responses as well as light adaptation in mammalian cones. Deletion of GCAPs increased 3-fold the amplitude and dramatically prolonged the light responses in dark-adapted mouse cones. It also reduced the operating range of mouse cones in background illumination and severely impaired their light adaptation. Thus, GCAPs exert powerful modulation on the mammalian cone phototransduction cascade and play an important role in setting the functional properties of cones in darkness and during light adaptation. Surprisingly, despite their better adaptation capacity and wider calcium dynamic range, mammalian cones were modulated by GCAPs to a lesser extent than mammalian rods. We conclude that a disparity in the strength of GCAPs modulation cannot explain the differences in the dark-adapted properties or in the operating ranges of mammalian rods and cones.

Keywords

Introduction

Rod and cone photoreceptors respond to over 10 logarithmic units of light intensities. Our ability to see over this enormous range can be explained, in part, by adaptation within rods and cones. Although the adaptation mechanisms that modulate rod phototransduction have

[3]Correspondencing authors: Vladimir Kefalov, Department of Ophthalmology and Visual Sciences, Washington University School of Medicine, 660 S. Euclid Ave, Campus Box 8096, St. Louis, MO 63110; Jeannie Chen, Zilkha Neurogenetic Institute, Keck School of Medicine, University of Southern California, 1501 San Pablo St, Rm. 223, Los Angeles, CA 90033. kefalov@vision.wustl.edu; jeannie@usc.edu.

been studied extensively (Burns and Arshavsky, 2005), the mechanisms that enable cones to adapt are poorly understood. Cone transduction proteins are homologous or identical to the ones found in rods and the cone phototransduction cascade is believed to function similarly to the one in rods (Ebrey and Koutalos, 2001). Yet remarkably, while rods saturate in moderately bright light (Green, 1971), cones can adjust their sensitivity and remain photosensitive even in bright light (Boynton and Whitten, 1970).

In both rods and cones, adaptation is modulated by changes in intracellular Ca^{2+}. In darkness, the continuous current entering the outer segment through the cGMP-gated channels is carried in part by Ca^{2+}, which is returned to the extracellular space via a $Na^+/(Ca^{2+}, K^+)$ exchanger. Following photoactivation and the closure of cGMP channels, the concentration of Ca^{2+} in the outer segment declines. This triggers a Ca^{2+}-mediated negative feedback on phototransduction which in rods mediates response shutoff and adaptation (Fain et al., 2001; Nakatani et al., 2002). Interestingly, Ca^{2+} constitutes a larger fraction of the total outer segment ionic flux in cones (20–35%) compared to rods (10–20%) (Korenbrot, 1995; Korenbrot and Rebrik, 2002). This attribute, in combination with the smaller outer segments of cones, allows their intracellular Ca^{2+} to decline several times faster upon light stimulation than that in rods (Sampath et al., 1999). In addition, the dynamic range of Ca^{2+} in cones is three-fold larger than that in rods (Korenbrot, 1995; Sampath et al., 1998; Sampath et al., 1999). Although these quantitative differences create the potential for stronger phototransduction modulation by Ca^{2+} in cones compared to rods, this issue has not been examined experimentally.

A key mechanism by which Ca^{2+} modulates phototransduction in rods involves the synthesis of cGMP by guanylyl cyclase (GC), regulated by a pair of Ca^{2+}-binding Guanylyl Cyclase Activating Proteins (GCAP1 and GCAP2) (Koch and Stryer, 1988; Burns et al., 2002). In rods, GCAPs modulate GC up to 20-fold, inhibiting it at high Ca^{2+} and activating it at low Ca^{2+} levels (Palczewski et al., 2000). The deletion of GCAPs in mouse rods abolishes the Ca^{2+} feedback on GC and results in slowed photoresponse shutoff and impaired light adaptation (Mendez et al., 2001; Burns et al., 2002). Electroretinogram recordings have provided an initial evidence for modulation of cone-driven bipolar cell responses by GCAPs (Pennesi et al., 2003). However, the effectiveness of GCAPs in modulating light response kinetics and sensitivity or their effect on light adaptation in mammalian cones has not been assessed. Here we addressed these questions by comparing the flash responses from control and GCAPs$^{-/-}$ mouse cones. Surprisingly, we found that while GCAPs strongly modulate cone sensitivity and response kinetics, the Ca^{2+} modulation on guanylyl cyclase is weaker in cones than in rods both in darkness and during light adaptation.

Materials and Methods

Animals

GCAPs knockout mice (GCAPs$^{-/-}$) (Mendez et al., 2001) of either sex were used after at least 12 hrs dark-adaptation. To facilitate suction recordings and to remove the rod component in the response of transretinal electroretinogram, all recordings for cones were done from mice in rod transducin alpha knockout (Gnat1$^{-/-}$) background (Calvert et al., 2000), generously provided by Janis Lem.

Western blot analysis

Retinas were dissected from mice at p30 and homogenized in buffer [80 mM Tris-HCl pH 8.0; 4 mM MgCl$_2$; protease inhibitor cocktail (Roche Diagnostics, Indianapolis, IN); and 0.5 mM phenylmethylsulfonyl fluoride (PMSF)], and incubated with DNase I (Roche

Diagnostics) for 30 – 45 min at room temperature. Equal volume of protein sample loading buffer (100 mM Tris, pH 6.8, 0.2 M dithiothreitol (DTT), 8% SDS, 20% glycerol, dash of bromophenol blue) was added, and the equivalent amounts of protein were loaded and separated in Tris-glycine polyacrylamide gel (Invitrogen Corp.). The protein samples then were transferred onto nitrocellulose membrane (Whatman Schleicher & Schuell) and were incubated with polyclonal antibodies against GCAP1, GCAP2, mouse green opsin (mGO), and rod transducin. The signal was detected using the Odyssey Infrared Imaging System from LI-COR Biosciences.

Immunofluorescence

All mice were killed at p30. Before enucleation, the superior pole for each mouse eye was cauterized for orientation. The mouse eye was placed in fixative solution (4.0% paraformaldehyde, 0.5% glutaraldehyde in 0.1M cacodylate buffer pH 7.2). The cornea and lens were removed, and the remaining eyecup was further fixed for 2 hrs and rinsed free of fixative with 0.1 M cacodylate buffer (pH 7.2). The tissues were infiltrated with 30% sucrose in 0.1M cacodylate buffer for 14–18 hrs at 4°C and embedded in Tissue Tek$^{®}$ O.C.T. (Sakura Kinetek U.S.A. Inc., Torrance, CA), and quickly frozen in liquid nitrogen. Ten micron frozen sections were obtained with a Jung CM 3000 cryostat machine (Leica Inc., Deerfield, IL). The retinal sections were incubated for 1 hour in blocking solution [2.0% BSA, 0.3% Triton X-100, and 2% goat serum in phosphate buffer saline (PBS)]. This blocking solution was also used in all subsequent antibody incubation steps. Some sections were incubated with mouse cone arrestin antibody (LUMI-J, (Zhu et al., 2002)). After washing with blocking solution, the sections were incubated with a 1:100 dilution of FITC-conjugated rabbit anti-mouse IgG (Vector Laboratories, Inc., Burlingame, CA). Other sections were incubated with fluorescein-conjugated peanut agglutinin (PNA, Vector Laboratories, Burlingame, CA). After a series of washing and a short fix (5 min in 4.0% paraformaldehyde in PBS), the sections were mounted with Vectashield containing DAPI (Vector Laboratories, Burlingame, CA), cover-slipped, and analyzed with an AxioPlan 2 imaging microscope (Carl Zeiss, Inc., Goettingen, Germany).

Electrophysiology

We performed single-cell suction recordings from individual cones and transretinal electroretinogram (ERG) recordings from isolated whole retina. Mice were maintained in 12/12hr light/dark cycle and dark-adapted overnight prior to experiments. Following euthanasia, eyes were marked for orientation, removed under dim red light, hemisected, and retinas were isolated under infrared light. For single-cell recordings, the dorsal part of retina was isolated, sliced with a razor blade, and stored in Locke solution at 4 °C. Recordings were done from small pieces of retina placed in a recording chamber fit to an inverted microscope and perfused at ~37 °C. The perfusion Locke solution contained 112 mM NaCl, 3.6 mM KCl, 2.4 mM $MgCl_2$, 1.2 mM $CaCl_2$, 10 mM HEPES, 20 mM $NaHCO_3$, 3 mM Na_2-succinate, 0.5 mM Na-glutamate, 10 mM glucose and was equilibrated with 95% O_2/5% CO_2, pH 7.4. For cones, recordings were done by drawing the cell body of a single photoreceptor into the recording electrode as previously described (Nikonov et al., 2006; Shi et al., 2007). The suction electrode was filled with solution containing 140 mM NaCl, 3.6 mM KCl, 2.4 mM $MgCl_2$, 1.2 mM $CaCl_2$, 3 mM HEPES, 10 mM glucose, pH 7.4. Responses were amplified by a current-to-voltage converter (Axopatch 200B; Molecular Devices, Sunnyvale, CA), low-pass filtered by an eight-pole Bessel filter (KROHN-HITE) with a cutoff frequency of 30 Hz, digitized at 1 kHz, and stored on a computer using pClamp 8.2 acquisition software (Molecular Devices). For BAPTA experiments, the retina was treated with Locke solution containing 100 μM BAPTA-AM for 20 min at room temperature.

For transretinal recordings, a quarter of the isolated dorsal retina was mounted on filter paper, photoreceptor-side up, and placed on the recording chamber with an electrode connected to the bottom. A second electrode was placed above the retina. To increase retina stability and the duration of recordings, the perfusion solution was kept at slightly lower temperature, ~34 °C, than for single-cell recordings. The perfusion Locke solution contained 2 mM L-glutamic acid to block higher order component of photoresponse (Sillman et al., 1969). The electrode solution under the retina contained, in addition, 10 mM $BaCl_2$ to suppress glial component (Bolnick et al., 1979; Nymark et al., 2005). Responses were amplified by a differential amplifier (DP-311; Warner Instruments). Saturated M-cone transretinal photoresponses were obtained using white light through a long-pass filter (>410 nm, Edmund GG455).

For all recordings and for all figures, test flashes were given at t = 0. Normalized flash sensitivity, S_F, was calculated as the ratio of dim-flash response amplitude and flash intensity normalized by the saturated dark-adapted response for each retina. Intensity-response data were fit by the equation:

$$\frac{R}{R_{\max}} = \frac{I}{I+I_o},$$

(1)

where R is the transient-peak amplitude of response, $R_{\max}$ is maximal response amplitude, I is flash intensity, and I_o is the flash intensity to generate half-maximal response.

The fractional amplitude of residual response in background illumination was fitted with Hill equation as follows:

$$\frac{R_{\max}}{R_{\max,dark}} = \frac{I_R^k}{I_R^k+I_B^k},$$

(2)

where R_{max} is a maximal response amplitude in background illumination, $R_{max,\ dark}$ is the maximal response amplitude in darkness, I_B(photons μm^{-2} s^{-1}) is the background light intensity, I_R (photons μm^{-2} s^{-1}) is the background light intensity required to reduce the amplitude two-fold, and k is the Hill coefficient.

The decline in photoreceptor sensitivity in background light was fit by the Weber-Fechner equation:

$$\frac{S_F}{S_F^D} = \frac{I_S}{I_S+I_B},$$

(3)

where S_F is photoreceptor sensitivity in background light, S_F^D is photoreceptor sensitivity in darkness, I_B (photons μm^{-2} s^{-1}) is the background light intensity, and I_S (photons $\mu m^{-2}s^{-1}$) is the background light intensity required to reduce sensitivity two-fold.

The expected exponential decline in sensitivity or residual maximal response in background, I_B, in the absence of adaptation was described as follows:

$$\frac{S_F}{S_F^D} = \frac{R_{\max}}{R_{\max,dark}} = \exp(-S_F^D T_i I_B),$$

(4)

where T_i (s) is the integration time of the dark-adapted response.

Estimation of collecting areas of cones

For suction recordings, as described previously (Baylor et al., 1979; Nikonov et al., 2005), the effective collecting area $a_c(\lambda)$ of the mouse cone for a flash of λ nm is given by the equation:

$$a_c(\lambda) = 2.303 \, f \, \varepsilon(\gamma) \, \gamma \, C \frac{\pi \, d^2 \, l_{cone}}{4} \times 10^{-4},$$

(5)

where f is a factor allowing for the use of unpolarized light entering the outer segment perpendicular to its axis ($f = 0.75$), $\varepsilon(\lambda)$ (M^{-1} cm^{-1}) is the extinction coefficient of M-opsin at a given wavelength λ (nm) of the pigment in solution, γ is the quantum efficiency of photoisomerization, C (M) is the pigment concentration in outer segment, and d (μm) and l_{cone} (μm) are the diameter and length of the outer segment. For M-opsin, $\varepsilon(500)$ and γ of M-opsin are 43,900 M^{-1} cm^{-1} and 0.61 (Sakurai et al., 2007) and the pigment concentration, C, is 3.2×10^{-3} M (Harosi, 1982). The cone outer segment has a base of 1.2 μm diameter, a tip of 0.8 μm diameter and a length of 13.4 μm (Carter-Dawson and LaVail, 1979). Thus, the estimated cone outer segment volume is 10.5 μm^3 assuming that its shape is equivalent to a cylinder with a diameter of 1.0 μm. Combining these values, the collection area, $a_c(500)$, of M-cones in our recording configuration is calculated as 0.16 μm^2.

For transretinal recordings, the effective collecting area $A_c(\lambda)$ of mouse M-cone for flash of λ nm is given by the equation:

$$A_c(\lambda) = k_f \frac{\pi \, d^2}{4} \left[1 - 10^{-\varepsilon(\lambda)Cl_{cone} \times 10^{-4}} \right] \gamma \, k_{shadow},$$

(6)

where d (μm) and l_{cone} (μm) are the diameter and length of the outer segments, respectively, k_f is a coefficient of funneling light effect ($k_f = 1$), and k_{shadow} denotes a coefficient, which represent the shadow effect of rod outer segments (Heikkinen et al., 2008). As the retina was placed on the chamber with photoreceptor side up, the shadow coefficient can be defined as $k_{shadow} = 10^{-(l_{rod} - l_{cone})\varepsilon_{rod}(500)C \times 10^{-4}}$, where l_{rod} (23.6 μm) and l_{cone} (13.4 μm) are the lengths of rod and cone outer segment, respectively. The molar extinction coefficient of mouse rhodopsin at 500 nm, $\varepsilon_{rod}(500)$, is 40,200 M^{-1} cm^{-1} (Imai et al., 2007). Thus, k_{shadow} can be estimated as 0.74 at 500 nm light. Our experiments were done using dorsal mouse retina, where M cones are dominant (Applebury et al., 2000). Assuming that transretinal photoresponses to green monochromatic light (500 nm) are derived from M-cones, we estimated $A_c(500)$ to be 0.12 μm^2.

Results

GCAPs$^{-/-}$, Gnat1$^{-/-}$ retina contains a normal complement of cones

GCAPs$^{-/-}$ mice (Mendez et al., 2001) were crossed with the Gnat1$^{-/-}$ mice lacking the alpha-subunit of rod transducin to facilitate the isolation of cone responses. The deletion of transducin renders the rods unable to respond to light while preserving the structure of rods and the morphology of the retina (Calvert et al., 2000). As both transducin and GCAPs are abundantly expressed in rod photoreceptors, we performed light microscopy on plastic embedded sections to evaluate whether the absence of these proteins affected retinal morphology. No changes were detected in the thickness of retinal layers and outer segment length (data not shown). We then performed immunocytochemistry on frozen sections to

determine whether the knockouts had a deleterious effect on cones. Retinal sections from wild type and knockout mice were reacted with mouse cone arrestin antibody (Nikonov et al., 2005) or peanut agglutinin, both of which label cones specifically (Fig. 1A). The labeled cones show similar density and outer segment morphology, and no difference was observed with respect to the number of cones counted in retinal sections that contain the entire span of retina along the vertical meridian (WT: 670 ± 10, n = 3; KO: 650 ± 10, n = 3; mean $\pm$ SEM). In addition, the level of mouse green opsin (mGO), another cone marker, was similar in retinal extracts from wild type and knockout mice (Fig. 1B). The absence of rod transducin-alpha (rTα) and the GCAPs proteins in the knockout mice was confirmed by western blots (Fig. 1B). Thus, removal of GCAPs and rod transducin had no discernable effect on cone morphology and on the expression of cone markers. This allowed us to use animals of rod transducin knockout background (Gnat1$^{-/-}$) to perform cone recordings as previously described (Nikonov et al., 2006; Shi et al., 2007) from control and GCAPs-deficient (GCAPs$^{-/-}$) animals.

GCAPs modulate the kinetics and sensitivity of single-cell cone responses

We began characterizing the role of GCAPs in mammalian cone phototransduction by investigating how their deletion affects the responses of mouse cones in dark-adapted conditions. To do that, we recorded suction electrode photoresponses to 500 nm test-flashes from single M-cones selected from the dorsal retina in Gnat1$^{-/-}$ mice (control cones) and in Gnat1$^{-/-}$ mice also lacking GCAPs (GCAPs$^{-/-}$ cones). Typical flash response families from control and GCAPs$^{-/-}$ cones are shown in Fig. 2A and 2B. The rising phase of the dim flash response in GCAPs$^{-/-}$ cones was not noticeably different from that in control cones (Fig. 2C), suggesting that GCAPs do not modulate the activation steps of cone phototransduction. However, the deletion of GCAPs had a dramatic effect on the kinetics of response shutoff. The lack of GCAPs delayed the onset of recovery (Fig. 2C, D) and increased the time to peak of mouse cone dim-flash responses by two-fold, from 112 ± 4 ms in control cones to 221 ± 9 ms in GCAPs$^{-/-}$ cones, respectively (Table 1). The effect of GCAPs deletion on the dim-flash integration time was even more dramatic as this parameter increased 3.3-fold from 112 ± 10 ms in control cones to 374 ± 23 ms in GCAPs$^{-/-}$ cones, respectively (Table 1).

The fractional response to a single cone pigment activation was $0.22 \pm 0.06\%$ (n = 12) of the total circulating current in control cones (Fig. 2C). This value is consistent with the ca. 0.2% obtained in previous studies (Nikonov et al., 2006; Heikkinen et al., 2008). In the absence of GCAPs, the fractional response increased ~3-fold to $0.63 \pm 0.14\%$ (n = 16) of the total circulating current in GCAPs$^{-/-}$ cones (Fig. 2C). Consistent with this increase in the single photon response, cone sensitivity also increased ~3-fold in GCAPs$^{-/-}$ cones compared to control cones as indicated by the corresponding decrease in half-saturating flash intensity (I_o) (Table 1). Together, these results indicate that the negative feedback on phototransduction by GCAPs strongly modulates the timely shutoff of the light response in mammalian cones and affects dramatically their response kinetics and sensitivity. Notably, the slower response recovery and increased single photon response in GCAPs$^{-/-}$ cones are qualitatively similar to the effects observed in GCAPs$^{-/-}$ rods (Burns et al., 2002). These results are also consistent with *in vivo* studies of cone function in GCAPs-deficient mice (Pennesi et al., 2003).

BAPTA has no effect on GCAPs$^{-/-}$ cones

To investigate whether other components, such as recoverin and calmodulin, modulate cone dim flash response kinetics in a calcium dependent manner, we pretreated control and GCAPs$^{-/-}$ mouse retinas with 100 μM BAPTA-AM to increase the buffering capacity of cone outer segments for Ca^{2+}. BAPTAtreatment slowed down substantially the kinetics of responses in control cones compared to untreated cones (Fig. 3A, Table 1) and often resulted

in overshoot or oscillation during their inactivation, indicating that BAPTA-AM was successfully incorporated into cone outer segments. This result is consistent with the deceleration of response shutoff in GCAPs$^{-/-}$ cones and indicates that Ca^{2+}-sensing proteins in cones are involved in modulating their dim flash response kinetics. In contrast, for GCAPs$^{-/-}$ cones the kinesics of BAPTA-treated responses did not differ from those of untreated GCAPs$^{-/-}$ cones (Fig. 3B, Table 1). Thus, in the dim flash regime, GCAPs appear to be the only calcium-dependent modulator of response kineticsin mouse cones.

GCAPs modulate the kinetics and sensitivity of transretinal cone responses

To characterize further the role of GCAPs in mammalian cone phototransduction, we next investigated how their deletion affects light adaptation of mouse cones. To do that, we performed transretinal cone recordings from isolated retinas of Gnat1$^{-/-}$ mice (control retinas) and Gnat1$^{-/-}$ mice also lacking GCAPs (GCAPs$^{-/-}$ retinas). Although this method produces responses with a waveform similar to that of single cell responses (Heikkinen et al., 2008; Wang and Kefalov, 2010), its major advantage over suction electrode recordings is that it provides stable and long-lasting recordings without significant deterioration of the responses for up to two hours. The glutamate in the perfusion solution (see **Materials and Methods** for details) saturated synaptic transmission to second order neurons and enabled us to observe the isolated response produced by photoreceptors without interference from second order neuron responses. We began by comparing the amplitudes and waveforms of flash responses from control and GCAPs$^{-/-}$ retinas under dark-adapted conditions (Fig. 4A and 4B) in experiments similar to the suction recordings described above. To avoid complications in the analysis, we used the dorsal part of the retina, populated predominantly with M-cones (Applebury et al., 2000; Haverkamp et al., 2005). As we used 500 nm light for stimulation, any response from S-cones would be expected to contribute to the overall response only at high enough intensities that overcome their low sensitivity in this part of the spectrum. This, in turn, would be expected to result in shallower and wider than normal intensity-response function (Eqn. (1)). However, the intensity-response measurements for both control and GCAPs$^{-/-}$ retinas were well fitted with Eqn. (1) (Fig. 4D), indicating the negligible contribution of S-opsin and S-cones to the photoresponses.

Similar to our findings from single-cell recordings above, the cone response kinetics of GCAPs$^{-/-}$ retinas were slower than those of control retinas (compare Fig. 4A and 4B). The cone response time to peak was increased two-fold, from 121 ± 4 ms in control retinas to 211 ± 5 ms in GCAPs$^{-/-}$ retinas (Table 2). The cone response integration time was also increased by more than 2.3-fold, from 183 ± 28 ms in controls retinas to 423 ± 21 ms in GCAPs$^{-/-}$ retinas (Table 2). Notably, the changes in cone response kinetics upon the deletions of GCAPs in transretinal (Table 2) and single-cell (Table 1) recordings were comparable. Furthermore, the fractional response by single cone pigment activation was $0.30 \pm 0.06\%$ (n = 13) of the maximum response in control retinas and ~3-fold higher in GCAPs$^{-/-}$ retinas at $0.83 \pm 0.12\%$ (n = 13) (Fig. 4C). These values are also comparable to the ones obtained with single-cell recordings. Consistent with the increase in the single photon response, the sensitivity of cones from GCAPs$^{-/-}$ retinas was also increased compared to that of cones from control retinas (Fig. 4D, Table 2). Together, these results indicate that the transretinal recordings from GCAPs-deficient cones yielded results essentially identical to the ones obtained using suction recordings. This validated our use of transretinal recordings to investigate the adaptation properties of control and GCAPs$^{-/-}$ cones described below.

GCAPs modulate the operating range of background illumination for cones

A key manifestation of light adaptation is the extension of the range of intensities over which the sensory cell can operate (Torre et al., 1995). In the absence of adaptation, the

maximum photoreceptor response declines exponentially with increasing background light and the cells rapidly saturate (Matthews et al., 1988). To determine the role of GCAPs in mammalian cone adaptation, we first investigated how their deletion affects the operating range of mouse cones. Figures 5A and 5B show typical cone responses from control and GCAPs$^{-/-}$ retinas, respectively, to steps of background light of increasing intensities. The background light caused a rapid response followed by a partial relaxation due to adaptation. The residual cone response in steady state was measured with a saturating test flash delivered 2 s after the onset of the background. As expected, the maximum response declined with increasing background light for both control and GCAPs$^{-/-}$ retinas (Fig. 5C). From Eqn. (2), the background intensity that reduced the maximum cone response two-fold (I_R) was 94,300 photons $\mu m^{-2}\,s^{-1}$ in control retinas and 3,900 photons $\mu m^{-2}\,s^{-1}$ in GCAPs$^{-/-}$ retinas (Table 2). Part of this 24-fold reduction could be attributed to the product of larger amplitude (2.7 fold) and longer integration time (2.3 fold) of the single photon responses of GCAPs$^{-/-}$ cones compared to controls, giving a total of 6.2-fold shift in the position of the operating range. The remaining 3.9-fold could be explained by compromised background adaptation of mouse cones in the absence of GCAPs. Notably, the decline of the maximum cone response amplitude with increasing background light was steeper in the absence of GCAPs (Fig. 5C) producing a change in the Hill coefficient of Eqn. (2) from 0.47 in control retinas to 0.70 in GCAPs$^{-/-}$ retinas (Table 2). The operating range of mouse cones, defined as the ratio of the background intensity at which the residual amplitude is 95% of its dark-adapted value and the intensity at which it is 5%, decreased from 2.8×10^5 fold to 4.5×10^3 fold upon deletion of GCAPs.

To confirm our findings from transretinal recordings, we performed limited background adaptation experiments from individual cones using a suction electrode. The response kinetics from single-cell recordings were somewhat faster than those from transretinal recordings, producing a slight shift of their adaptation curves (Fig. 5, inset) to the right compared to those from transretinal recordings. This was most likely due to the difference in recording temperature: the single-cell recordings were done at 37 °C vs. 34 °C for the transretinal recordings (this lower temperature was used in order to improve the stability and length of the transretinal recordings). Notably however, the shift in the single-cell adaptation curve induced by GCAPs deletion was 28-fold, comparable to that measured with transretinal recordings. In addition, the values for the Hill coefficient, k, measured from these recordings, 0.49 and 0.78 for control and GCAPs$^{-/-}$ cones, respectively, were comparable to those measured from transretinal recordings (Table 2). Together, these results demonstrate that Ca^{2+} modulation of GC activity via GCAPs plays an important role in shifting the operating range of mammalian cones to brighter light and in widening their adaptation curve.

Deletion of GCAPs impairs cone light adaptation

To further characterize the role of GCAPs in mammalian cone adaptation, we next investigated how their deletion affects the light sensitivity of mouse cones. We used an experimental protocol similar to the one described above, but now measured sensitivity by recording the cone dim flash responses 2 s after the onset of step light of various intensity in control (Fig. 6A) and GCAPs$^{-/-}$ (Fig. 6B) retinas. In both cases, the cone dim flash response amplitude gradually decreased with increasing background light intensity. Cone flash sensitivity (S_F) decline in control and GCAPs$^{-/-}$ retinas could be fitted with the Weber-Fechner function (Eqn. (3); Fig. 6C). The background light required to reduce cone sensitivity two-fold (I_S) declined by 12-fold, from 12,900 photons $\mu m^{-2}\,s^{-1}$ for control retina to 1,100 photons $\mu m^{-2}\,s^{-1}$ for GCAPs$^{-/-}$ retina (Table 2). The dim flash response used to estimate cone sensitivity was not greater than 30% of the maximum for all backgrounds in both genotypes except for the two brightest backgrounds in GCAPs$^{-/-}$

retinas. There, the responses to dimmer flashes would have been too small to measure reliably due to response compression, and we were forced to use slightly higher flash intensity, producing 35% and 42% fractional responses. This likely explains the underestimation of GCAPs$^{-/-}$ cone sensitivity at backgrounds $> 2 \times 10^3$ photons μm^{-2} s^{-1} (Fig. 6C). Notably, the initial desensitization of GCAPs$^{-/-}$ cones in background light followed the expected change in sensitivity in the absence of adaptation (Eqn. (4); Fig. 6C, dotted line). Thus, the calcium modulation of GC is the dominant mechanism for mammalian cone adaptation in dim to moderate background light conditions.

One complication of our analysis was the larger single photon response amplitude and larger integration time of GCAPs$^{-/-}$ cones which increased the effective activation by steady light in GCAPs$^{-/-}$ compared to control retinas (Fig. 5C). To exclude this effect on the flash sensitivity change, we plotted the normalized cone sensitivity (S_F/S_F^D) against the normalized maximal residual amplitude (Fig. 6D). Considering that the internal calcium concentration declines proportionally to the residual photoreceptor dark current (Sampath et al., 1999; Matthews and Fain, 2003), the normalized residual response, $R_{max}/R_{max, dark}$, must be proportional to the relative change in calcium (Ca^{2+}/Ca^{2+}_{dark}). Notably, GCAPs$^{-/-}$ cones desensitized less than control cones for equal decline in calcium levels (Fig. 6D). These results indicate that the deletion of GCAPs compromises the ability of cones to lower their sensitivity in adaptation to background light.

GCAPs and light adaptation in rods vs. cones

The effects of GCAPs deletion on light adaptation in mouse rods has been characterized previously (Mendez et al., 2001). To compare the roles of GCAPs in adaptation in rods vs. cones, we repeated and extended these rod experiments using the same transretinal recording protocols described above for cones. Similar to the case of cones, the maximum response of light adapted rods declined with increasing background light for both wild type control and GCAPs$^{-/-}$ retinas (Fig. 7A). The operating range of mouse rods spanned 140-fold of background light (Fig. 7A). This is 2000-fold less than the corresponding 2.8×10^5-fold operating range of cones (Fig. 5C). The background intensity that reduced the maximum rod response 2-fold from its dark-adapted level (I_R) was 756 photons μm^{-2} s^{-1} in control rods and 27 photons μm^{-2} s^{-1} in GCAPs$^{-/-}$ rods (Table 3), indicating that 28-fold shift was induced by the deletion of GCAPs in rods. As in cones, part of this shift could be attributed to the increase in dark-adapted sensitivity (3.5-fold) and integration time (3.1-fold) upon the deletion of GCAPs in rods, giving a total of 11-fold difference (also larger than the corresponding 6.2-fold difference in cones). The remaining 2.5-fold (28/11) shift in the operating range to lower intensities could be explained by impaired rod adaptation. Notably, in contrast to the case in cones, the deletion of GCAPs in rods did not affect the Hill coefficient of their Weber-Fechner curve (Fig. 7A; Table 3). Thus, unlike in cones, in rods the Ca^{2+} modulation of GC activity via GCAPs does not widen their adaptation curve and its effect is restricted to shifting the operating range of rods to brighter light.

The impaired adaptation of GCAPs-deficient rods could also be observed from the shift in normalized flash sensitivity (S_F/S_F^D) in GCAPs$^{-/-}$ retinas (Fig. 7B). The background light required to reduce rod sensitivity two-fold (I_S) in control retinas was 272 photons μm^{-2} s^{-1} (Table 3). Taking into account the ~30% smaller photoreceptor collecting area for transretinal recordings compared to single-cell recordings (see **Materials and Methods** for details), this value is comparable to the 159 photons μm^{-2} s^{-1} value, measured from single-cell recordings (Mendez et al., 2001). The deletion of GCAPs resulted in 18-fold reduction of rod I_S to 14 photons μm^{-2} s^{-1} (Fig. 7B, Table 3). To determine the effect of background on flash sensitivity independent of the change in maximum response amplitude, we again plotted the normalized sensitivity against the residual maximal amplitude for control and GCAPs$^{-/-}$ rods (Fig. 7C, solid lines). We then compared the adaptation in rods with the

results obtained from cones, replotted from Fig. 6D (Fig 7C, dashed lines). For comparison we also included the expected decline in relative sensitivity in the absence of any Ca^{2+}-modulation (Fig. 7C, blue dotted line). The extent of Ca^{2+}-modulation for each photoreceptor could be quantified by the shift in the slope of the corresponding fitting power functions. Thus, the contribution of GCAPs to Ca^{2+}-modulation in rods could be estimated as 0.7 by dividing the power function of GCAPs$^{-/-}$ rods (solid red line) by the power function of control rods (solid black line). This ratio, 1.7/2.3, indicated that 30% of the flash sensitivity decline in rods could be attributed to GCAPs feedback. Notably, the contribution of GCAPs to Ca^{2+}-modulation in cones, estimated by dividing the corresponding power functions of GCAPs$^{-/-}$ cones (dashed red line) and control cones (dashed black line), was 0.8 (2.4/2.9), indicating that only 20% of the flash sensitivity decline in cones could be attributed to GCAPs feedback. Thus, the extent of Ca^{2+}-dependent modulation on adaptation by GCAPs appears to be larger in mammalian rods than that in cones.

Discussion

Our analysis of the function of GCAPs-deficient mouse cones demonstrates that the Ca^{2+} feedback to guanylyl cyclase regulates mammalian cone flash response sensitivity and kinetics in darkness and during light adaptation. Block of this modulation in mouse cones by the deletion of GCAP1 and GCAP2 increased the fractional flash response 3-fold compared to control cones. While the rising phase of the dim flash response was not affected by the lack of GCAPs modulation, the shutoff of the response was severely delayed, with a 2-fold longer time to peak and 3-fold longer integration time. Block of the Ca^{2+} feedback mediated by GCAPs also shifted by 24-fold the operating range of cones to lower background lights and narrowed their adaptation curve. Most (6.2-fold) of the reduction in the cone operating range could be explained by the increase in single photon response amplitude and integration time of GCAPs-deficient cones compared to controls. Comparison of the effects of GCAPs deletion in mammalian rods and cones revealed that, surprisingly, the Ca^{2+} modulation on guanylyl cyclase is weaker in cones than in rods both in darkness and during light adaptation.

GCAPs is required for the timely response shutoff in mammalian cones

The decline in calcium induced by light could modulate phototransduction through at least three different feedback mechanisms affecting shutoff of the photoactivated pigment, the conductance of the cGMP channels, and the synthesis of cGMP. For rods, the Ca^{2+}-dependent modulation of cGMP synthesis by GC is dominant in dim light conditions (Koutalos and Yau, 1996; Burns et al., 2002; Makino et al., 2004). In contrast, modulation of the photoactivated pigment (Burns et al., 2002; Makino et al., 2004) and the cGMP-gated channels (Chen et al., 2010) play no detectable role in rod background light adaptation. Our finding that BAPTA fails to slow down the response of GCAP$^{-/-}$ cones (Fig. 3B) indicates that, similar to the case in rods, GCAPs modulation on the synthesis of cGMP is the major mechanism controlling the timely shutoff of dim flash responses in mammalian cones.

Comparison of dim flash transretinal responses from control and GCAPs-deficient photoreceptors allowed us to estimate and compare the times of onset of the calcium modulation of GC following a flash in rods and cones. In rods, the GCAPs-deficient responses began deviating from control responses ~120 ms after the flash (Fig 7D). In cones, the two responses deviated at ~80 ms. Thus, consistent with the expected faster decline of calcium in cones compared to rods (Sampath et al., 1999), the onset of their GCAPs modulation was also faster. Interestingly, this 1.4-fold (120/80) slower onset of the GCAPs feedback in rods vs. cones was comparable with the 1.5-fold (163/121) larger time to peak of rods vs. cones (Tables 2 and 3). Thus, the difference in time to peak between rods and

cones could possibly be due to the slower onset of the GCAPs feedback in rods compared to cones.

Weaker GCAPs modulation in cones than in rods

Our study clearly demonstrates that Ca^{2+}-dependent modulation of cGMP synthesis by GCAPs affects the dark-adapted response kinetics and sensitivity as well as the adaptation capacity of mammalian cones. Considering the wider functional range of cones compared to rods, we expected that Ca^{2+}-dependent modulation of GCAPs in cones will be stronger than that in rods. Yet, surprisingly, the strength of the modulation by GCAPs in dark-adapted state appears to be lower in cones than in rods. Thus, deletion of GCAPs resulted in only 2–3 fold increase in single photon response amplitude in mouse cones (Figs. 2C and 4C) compared to a corresponding 5–6 fold increase in mouse rods (Mendez et al., 2001). Another way of comparing the strength of GCAPs modulation in rods and cones is by estimating the feedback loop gain, gL, as previously described (Burns et al., 2002). For small responses that cause linear perturbations in the loop $\gamma L = 1 + gL$, where γL is the ratio of time integrals of single photon response in $GCAPs^{-/-}$ and control cones. The ratio of single photon responses in $GCAPs^{-/-}$ and control cones was 2.9 (0.63/0.22; see Results) and the corresponding ratio of integration times was 3.3 (374/112; Table 2). Thus, the time integral of the $GCAPs^{-/-}$ cone responses was 9.6-fold larger than that of control cone responses. This gave a value for γL of 9.6, and a cone feedback loop gain of 8.6. Notably, this value is lower than the corresponding strength of the feedback loop in rods, previously estimated to be 11 (Burns et al., 2002). Together, these results rule out differences in the strength of feedback on cGMP synthesis as a possible mechanism contributing to the lower sensitivity of mammalian cones compared to rods.

The strength of the modulation by GCAPs was comparable or perhaps even slightly lower in mouse cones than in rods during background adaptation. The deletion of GCAPs induced a 24-fold shift to lower intensities in the operating range in mouse cones (Fig. 5C and Table 2), compared to a corresponding 28-fold shift in mouse rods (Fig. 7B and Table 3). The relatively weak contribution of GCAPs modulation to light adaptation in cones compared to rods was confirmed by the smaller shift in the relative sensitivity vs. residual maximal response function upon the deletion of GCAPs (Fig. 7C) for cones (20%) compared to rods (30%). These results also indicate that though the Ca^{2+} feedback on GC is the main mechanism for mammalian cone background adaptation for dim to moderate light intensities (Fig. 6C), other mechanisms dominate adaptation in brighter light conditions.

One notable difference between rods and cones was how the deletion of GCAPs affected their operating range. In rods, the deletion of GCAPs resulted in a simple shift of the adaptation curve without affecting its Hill coefficient (Fig. 7A and Table 3). In contrast, in cones the deletion of GCAPs not only shifted their adaptation curve but also accelerated cone saturation as demonstrated by the higher Hill coefficient of adaptation (Fig. 5C and Table 2). Thus, GC modulation by GCAPs hinders saturation and widens the operating range in mammalian cones but not in rods.

Rod vs. cone isoforms of GC and GCAPs

A possible explanation for the differences in strength of the Ca^{2+} feedback on cGMP synthesis in rods and cones could be the expression of rod/cone specific isoforms of GC and GCAPs or the coexpression of their isoforms with different ratios in rods and cones. For instance, carp rods and cones express different isoforms of GC (GC-R1 and GC-R2 in rods vs. GC-C in cones) and GCAPs (GCAP1 and GCAP2 in rods vs. GCAP3 in cones) (Takemoto et al., 2009). This would allow for photoreceptor-specific tuning of the modulation of cGMP synthesis in rods vs. cones. In contrast, rods and cones in the mouse

share the same isoforms of GC and GCAPs (Howes et al., 1998). However, mouse cones primarily express GC1 and GCAP1 (Cuenca et al., 1998) whereas mouse rods express both isoforms of GC (GC1 and GC2) and GCAP (GCAP1 and GCAP2) (Cuenca et al., 1998; Baehr and Palczewski, 2007). It is possible, therefore, that differences in the Ca^{2+} sensitivities of GCAP1 and GCAP2 and in the way that they modulate GC1 and GC2 (Peshenko and Dizhoor, 2004) account for the rod/cone differences in modulation of cGMP synthesis. Notably, the GCAP2 modulation of guanylyl cyclase in rods becomes more prominent at higher intensities of background light (Makino et al., 2008). This observation is consistent with our finding that the overall modulation of guanylyl cyclase is weaker in mouse cones, which express primarily GCAP1, than in mouse rods, where GCAP2 is expressed more abundantly.

Another possibility is that the expression levels of GC and GCAPs differ in rods and cones. Indeed, in the case of carp retina, the expression of both GC and GCAPs is significantly higher in cones compared to rods (Takemoto et al., 2009) and the basal activity of GC in cones is 36-fold higher than that in rods. In addition to the rod/cone differences in GC and GCAPs expression, this higher activity of GC in dark-adapted cones might be due to a lower level of dark-adapted Ca^{2+} in cones compared to rods (Sampath et al., 1998; Sampath et al., 1999). A higher dark-adapted activity of GC (and concomitant higher dark PDE activity) would restrict the range of upregulation of cGMP synthesis upon illumination in cones compared to rods. Consistent with this notion, the incremental GC activity in carp rods at a low Ca^{2+} concentration, namely in light-adapted conditions, increases by a factor of 7 compared to that at a high Ca^{2+} concentration, namely in darkness, whereas the GC activity in cones in light-adapted conditions is raised by only 2-fold compared to that in darkness (Takemoto et al., 2009). This observation is consistent with our results indicating a smaller contribution of GCAPs modulation to light adaptation in cones compared to that in rods. Thus, the wide range of adaptation in cones could be accomplished by the Ca^{2+}-mediated modulation of photoactivated pigment lifetime, cGMP channel conductance, or by additional, yet unknown mechanisms.

Acknowledgments

References

Applebury ML, Antoch MP, Baxter LC, Chun LL, Falk JD, Farhangfar F, Kage K, Krzystolik MG, Lyass LA, Robbins JT. The murine cone photoreceptor: a single cone type expresses both S and M opsins with retinal spatial patterning. Neuron. 2000; 27:513–523. [PubMed: 11055434]

Baehr W, Palczewski K. Guanylate cyclase-activating proteins and retina disease. Subcell Biochem. 2007; 45:71–91. [PubMed: 18193635]

Baylor DA, Lamb TD, Yau KW. Responses of retinal rods to single photons. J Physiol. 1979; 288:613–634. [PubMed: 112243]

Bolnick DA, Walter AE, Sillman AJ. Barium suppresses slow PIII in perfused bullfrog retina. Vision Res. 1979; 19:1117–1119. [PubMed: 317765]

Boynton RM, Whitten DN. Visual adaptation in monkey cones: recordings of late receptor potentials. Science. 1970; 170:1423–1426. [PubMed: 4991522]

Burns ME, Arshavsky VY. Beyond counting photons: trials and trends in vertebrate visual transduction. Neuron. 2005; 48:387–401. [PubMed: 16269358]

Burns ME, Mendez A, Chen J, Baylor DA. Dynamics of cyclic GMP synthesis in retinal rods. Neuron. 2002; 36:81–91. [PubMed: 12367508]

Calvert PD, Krasnoperova NV, Lyubarsky AL, Isayama T, Nicolo M, Kosaras B, Wong G, Gannon KS, Margolskee RF, Sidman RL, Pugh EN Jr, Makino CL, Lem J. Phototransduction in transgenic mice after targeted deletion of the rod transducin alpha -subunit. Proc Natl Acad Sci U S A. 2000; 97:13913–13918. [PubMed: 11095744]

Carter-Dawson LD, LaVail MM. Rods and cones in the mouse retina. I. Structural analysis using light and electron microscopy. J Comp Neurol. 1979; 188:245–262. [PubMed: 500858]

Chen JC, Woodruff ML, Wang T, Concepcion FA, Tranchina D, Fain GL. Channel modulation and the mechanism of light adaptation in mouse rods. J Neurosci. 2010 (in press).

Cuenca N, Lopez S, Howes K, Kolb H. The localization of guanylyl cyclase-activating proteins in the mammalian retina. Invest Ophthalmol Vis Sci. 1998; 39:1243–1250. [PubMed: 9620085]

Ebrey T, Koutalos Y. Vertebrate photoreceptors. Prog Retin Eye Res. 2001; 20:49–94. [PubMed: 11070368]

Fain GL, Matthews HR, Cornwall MC, Koutalos Y. Adaptation in vertebrate photoreceptors. Physiol Rev. 2001; 81:117–151. [PubMed: 11152756]

Green DG. Light adaptation in the rat retina: evidence for two receptor mechanisms. Science. 1971; 174:598–600. [PubMed: 5114823]

Harosi FI. Polarized microspectrophotometry for pigment orientation and concentration. Methods Enzymol. 1982; 81:642–647. [PubMed: 7098904]

Haverkamp S, Wassle H, Duebel J, Kuner T, Augustine GJ, Feng G, Euler T. The primordial, blue-cone color system of the mouse retina. J Neurosci. 2005; 25:5438–5445. [PubMed: 15930394]

Heikkinen H, Nymark S, Koskelainen A. Mouse cone photoresponses obtained with electroretinogram from the isolated retina. Vision Res. 2008; 48:264–272. [PubMed: 18166210]

Howes K, Bronson JD, Dang YL, Li N, Zhang K, Ruiz C, Helekar B, Lee M, Subbaraya I, Kolb H, Chen J, Baehr W. Gene array and expression of mouse retina guanylate cyclase activating proteins 1 and 2. Invest Ophthalmol Vis Sci. 1998; 39:867–875. [PubMed: 9579466]

Imai H, Kefalov V, Sakurai K, Chisaka O, Ueda Y, Onishi A, Morizumi T, Fu Y, Ichikawa K, Nakatani K, Honda Y, Chen J, Yau KW, Shichida Y. Molecular properties of rhodopsin and rod function. J Biol Chem. 2007; 282:6677–6684. [PubMed: 17194706]

Koch KW, Stryer L. Highly cooperative feedback control of retinal rod guanylate cyclase by calcium ions. Nature. 1988; 334:64–66. [PubMed: 2455233]

Korenbrot JI. Ca2+ flux in retinal rod and cone outer segments: differences in Ca2+ selectivity of the cGMP-gated ion channels and Ca2+ clearance rates. Cell Calcium. 1995; 18:285–300. [PubMed: 8556768]

Korenbrot JI, Rebrik TI. Tuning outer segment Ca2+ homeostasis to phototransduction in rods and cones. Adv Exp Med Biol. 2002; 514:179–203. [PubMed: 12596922]

Koutalos Y, Yau KW. Regulation of sensitivity in vertebrate rod photoreceptors by calcium. Trends Neurosci. 1996; 19:73–81. [PubMed: 8820871]

Makino CL, Peshenko IV, Wen XH, Olshevskaya EV, Barrett R, Dizhoor AM. A role for GCAP2 in regulating the photoresponse. Guanylyl cyclase activation and rod electrophysiology in GUCA1B knock-out mice. J Biol Chem. 2008; 283:29135–29143. [PubMed: 18723510]

Makino CL, Dodd RL, Chen J, Burns ME, Roca A, Simon MI, Baylor DA. Recoverin regulates light-dependent phosphodiesterase activity in retinal rods. J Gen Physiol. 2004; 123:729–741. [PubMed: 15173221]

Matthews HR, Fain GL. The effect of light on outer segment calcium in salamander rods. J Physiol. 2003; 552:763–776. [PubMed: 12949220]

Matthews HR, Murphy RL, Fain GL, Lamb TD. Photoreceptor light adaptation is mediated by cytoplasmic calcium concentration. Nature. 1988; 334:67–69. [PubMed: 2455234]

Mendez A, Burns ME, Sokal I, Dizhoor AM, Baehr W, Palczewski K, Baylor DA, Chen J. Role of guanylate cyclase-activating proteins (GCAPs) in setting the flash sensitivity of rod photoreceptors. Proc Natl Acad Sci U S A. 2001; 98:9948–9953. [PubMed: 11493703]

Nakatani K, Chen C, Yau KW, Koutalos Y. Calcium and phototransduction. Adv Exp Med Biol. 2002; 514:1–20. [PubMed: 12596912]

Nikonov SS, Kholodenko R, Lem J, Pugh EN Jr. Physiological Features of the Sand M-cone Photoreceptors of Wild-type Mice from Single-cell Recordings. J Gen Physiol. 2006; 127:359–374. [PubMed: 16567464]

Nikonov SS, Daniele LL, Zhu X, Craft CM, Swaroop A, Pugh EN Jr. Photoreceptors of Nrl −/− mice coexpress functional S- and M-cone opsins having distinct inactivation mechanisms. J Gen Physiol. 2005:287–304. [PubMed: 15738050]

Nymark S, Heikkinen H, Haldin C, Donner K, Koskelainen A. Light responses and light adaptation in rat retinal rods at different temperatures. J Physiol. 2005; 567:923–938. [PubMed: 16037091]

Palczewski K, Polans AS, Baehr W, Ames JB. Ca(2+)-binding proteins in the retina: structure, function, and the etiology of human visual diseases. Bioessays. 2000; 22:337–350. [PubMed: 10723031]

Pennesi ME, Howes KA, Baehr W, Wu SM. Guanylate cyclase-activating protein (GCAP) 1 rescues cone recovery kinetics in GCAP1/GCAP2 knockout mice. Proc Natl Acad Sci U S A. 2003; 100:6783–6788. [PubMed: 12732716]

Peshenko IV, Dizhoor AM. Guanylyl cyclase-activating proteins (GCAPs) are Ca2+/Mg2+ sensors: implications for photoreceptor guanylyl cyclase (RetGC) regulation in mammalian photoreceptors. J Biol Chem. 2004; 279:16903–16906. [PubMed: 14993224]

Sakurai K, Onishi A, Imai H, Chisaka O, Ueda Y, Usukura J, Nakatani K, Shichida Y. Physiological properties of rod photoreceptor cells in green-sensitive cone pigment knock-in mice. J Gen Physiol. 2007; 130:21–40. [PubMed: 17591985]

Sampath AP, Matthews HR, Cornwall MC, Fain GL. Bleached pigment produces a maintained decrease in outer segment Ca2+ in salamander rods. J Gen Physiol. 1998; 111:53–64. [PubMed: 9417134]

Sampath AP, Matthews HR, Cornwall MC, Bandarchi J, Fain GL. Light-dependent changes in outer segment free-Ca2+ concentration in salamander cone photoreceptors. J Gen Physiol. 1999; 113:267–277. [PubMed: 9925824]

Shi G, Yau KW, Chen J, Kefalov VJ. Signaling properties of a short-wave cone visual pigment and its role in phototransduction. J Neurosci. 2007; 27:10084–10093. [PubMed: 17881515]

Sillman AJ, Ito H, Tomita T. Studies on the mass receptor potential of the isolated frog retina. I. General properties of the response. Vision Res. 1969; 9:1435–1442. [PubMed: 5367433]

Takemoto N, Tachibanaki S, Kawamura S. High cGMP synthetic activity in carp cones. Proc Natl Acad Sci U S A. 2009; 106:11788–11793. [PubMed: 19556550]

Torre V, Ashmore JF, Lamb TD, Menini A. Transduction and adaptation in sensory receptor cells. J Neurosci. 1995; 15:7757–7768. [PubMed: 8613717]

Wang JS, Kefalov VJ. Single-cell suction recordings from mouse cone photoreceptors. J Vis Exp. 2010

Zhu X, Li A, Brown B, Weiss ER, Osawa S, Craft CM. Mouse cone arrestin expression pattern: light induced translocation in cone photoreceptors. Mol Vis. 2002; 8:462–471. [PubMed: 12486395]
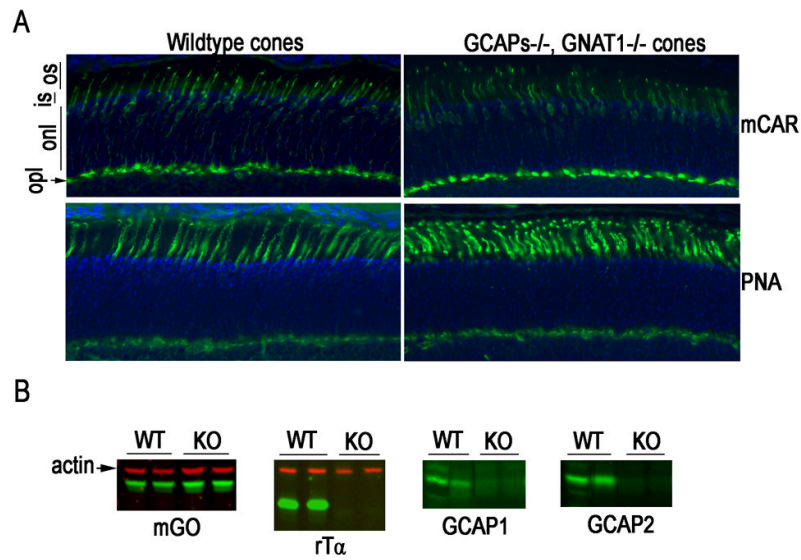
Figure 1.
Cone density and expression of transduction proteins in wild type and GCAPs$^{-/-}$, GNAT1$^{-/-}$ retina. Cones were visualized by immunofluorescence (green) (A) of mouse cone arrestin (mCAR, upper panel) and peanut agglutinin (PNA, lower panel). Nuclei were stained with DAPI (blue). Abbreviations: os, outer segment; is, inner segment; onl, outer nuclear layer; opl, outer plexiform layer. (B) Representative western blots of whole retinal homogenate from wild type and GCAPs$^{-/-}$, GNAT1$^{-/-}$ mice probed with antibodies against the indicated transduction protein (mGO, mouse green opsin; rTα, rod transducin alpha; GCAP1 and GCAP2). Actin served as a loading control. Each lane contains retinal homogenate from a different mouse. No changes in expression level of mouse green opsin were observed.
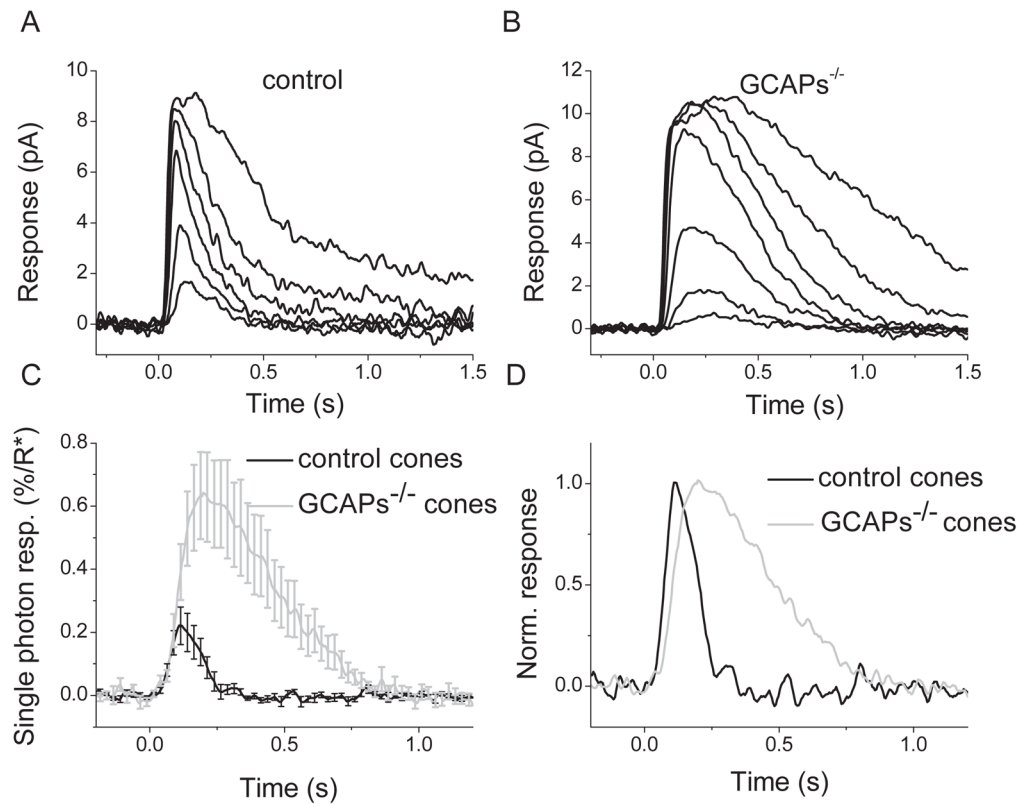
Figure 2.
Flash response families of dark adapted control (A) and GCAPs$^{-/-}$ (B) M-cones recorded with a suction electrode. Cone responses were evoked by a series of 500-nm test flashes (10 ms in duration). The test flash intensities (in photons μm^{-2}) were 500, 1.4×10^3, 5.7×10^3, 1.9×10^4, 5.2×10^4, and 1.7×10^5 for control cones, and 180, 500, 1.4×10^3, 5.7×10^3, 1.9×10^4, 5.2×10^4, and 1.7×10^5 for GCAPs$^{-/-}$ cones. (C) Averaged single photon responses of control (black, n = 12) and GCAPs$^{-/-}$ (gray, n = 16) cones. Error bars show SEM. To calculate the number of R*, the collecting area of cones was estimated to be 0.16 μm^2 (see Eqn. (5) and **Materials and Methods** for details). (D) The responses from (C) replotted normalized to unity to demonstrate the slower response kinetics of the GCAPs$^{-/-}$ cones (grey) compared to control cones (black).
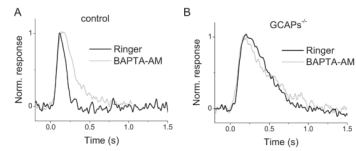
Figure 3.
Lack of effect by BAPTA on GCAPs$^{-/-}$ cone response kinetics. Normalized dim flash responses from control (A) and GCAPs$^{-/-}$ (B) cones. Black traces show responses in control solution and gray traces show responses from cones treated with 100 μM BAPTA-AM.
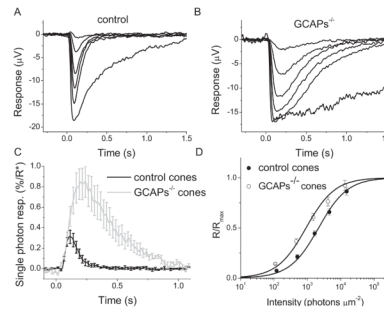
Figure 4.
Flash response families of dark adapted control cones (A) and GCAPs$^{-/-}$ cones (B) from transretinal recordings. Cone responses were evoked by a series of 500-nm test flashes (10 ms in duration) with intensities (photons μm^{-2}) 36, 1.2×10^2, 3.9×10^2, 1.1×10^3, and 3.6×10^3. The largest response in each case was triggered by unattenuated white flash. (C) Fractional single photon responses of control (black) and GCAPs$^{-/-}$ (gray) cones. Error bars show SEM. The cone collecting area was estimated to be 0.12 μm^2 (see Eqn. (6) and **Materials and Methods** for details). (D) Intensity-response relations of cone transretinal responses to estimate sensitivity in control (closed circles) and GCAPs$^{-/-}$(open circles) retinas. The solid curves represent the corresponding intensity-response functions (Eqn. (1)) with I$_o$ of 2,180 photons μm^{-2} and 918 photons μm^{-2}, respectively. Error bars show SEM.
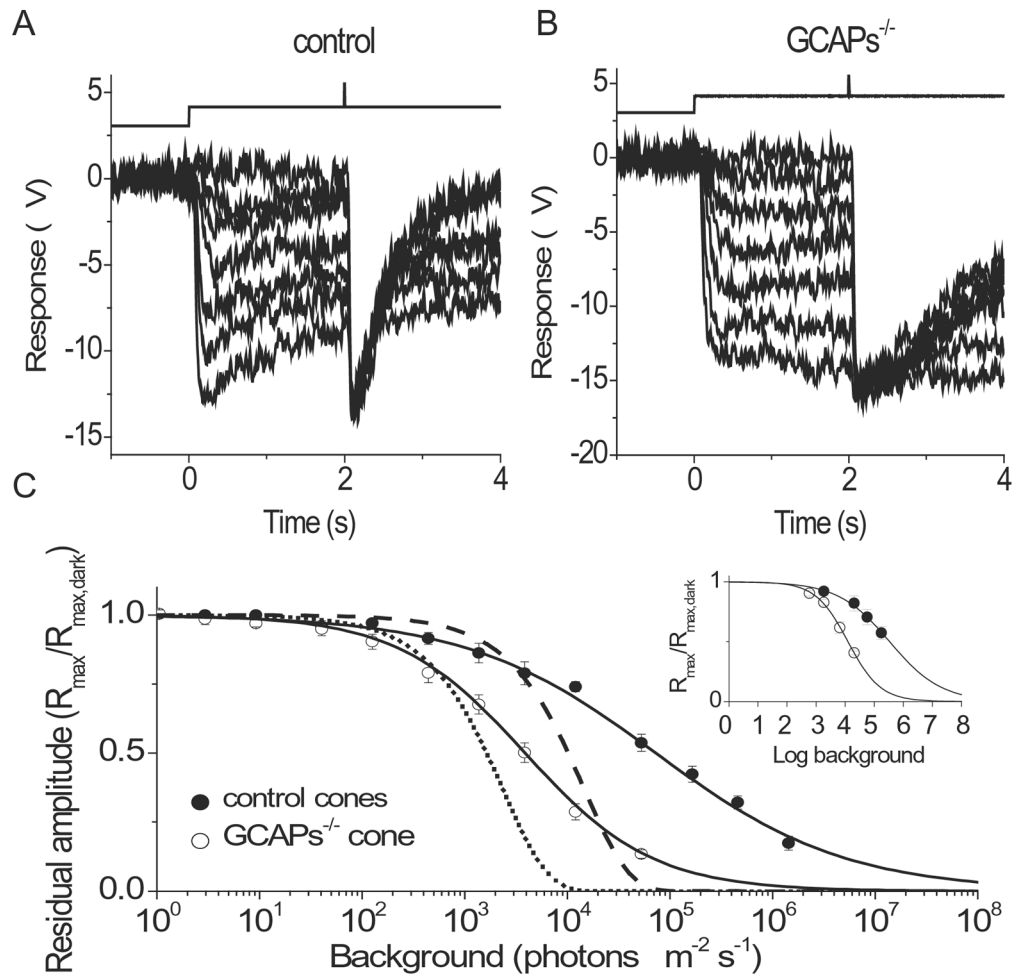
Figure 5.
Effect of background light on cone operating range in control and GCAPs$^{-/-}$ retinas. Maximum cone response amplitudes under a series of background lights were measured 2 s after the onset of step light illumination in control (A) and GCAPs$^{-/-}$ (B) retinas by a test flash of unattenuated white light. The time course of light stimulation is shown on the top of each panel. The step light intensities (photons $\mu m^{-2} s^{-1}$) were 0, 440, 1.3×10^3, 3.9×10^3, 1.2×10^4, 5.2×10^4, and 1.7×10^5 for control retina and 0, 130, 440, 1.3×10^3, 3.9×10^3, 1.2×10^4, and 5.2×10^4 for GCAPs$^{-/-}$ retina. (C) Normalized maximum cone responses as a function of background intensity for control (filled circles) and GCAPs$^{-/-}$ (open circles) retina. The smooth curves represent best-fitted Hill equation (see Eqn. (2)) with k = 0.47 and 0.70, I_R = 94,300 and 3,900 photons $\mu m^{-2} s^{-1}$ for control and GCAPs$^{-/-}$, respectively. Error bars show SEM. The dashed and dotted curves represent the expected change in maximum response of control and GCAPs$^{-/-}$ cones, respectively, in the absence of adaptation (see Eqn. (4)). (Inset) Normalized maximum cone response as a function of background intensity for control (n = 5) and GCAPs$^{-/-}$ (n = 5) cones obtained with single-cell recordings. The curves represent best-fitted Hill equations with k = 0.49 and 0.78, I_R = 3.4×10^5 and 1.2×10^4 photons $\mu m^{-2} s^{-1}$ for control and GCAPs$^{-/-}$ cones, respectively.
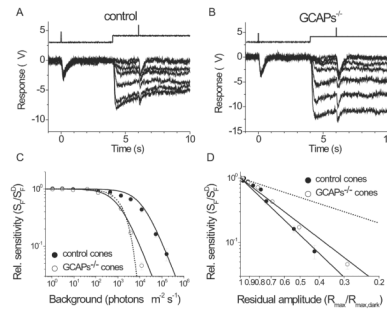
Figure 6.
Effect of background light on cone sensitivity in control and GCAPs$^{-/-}$ retinas. Sensitivity under a series of background lights was measured from dim flash responses delivered 2 s after the onset of step light illumination in control (A) and GCAPs$^{-/-}$ (B) retinas. The time course of light stimulation is shown on the top of each panel. The flash intensities (photons μm^{-2}) delivered in darkness for control and GCAPs$^{-/-}$ retinas were 1.6×10^3 and 120, respectively. The flash intensities (photons μm^{-2}) delivered on the step light for control retina were 1.6×10^3 for the first 5 traces, 4.5×10^3, and 1.5×10^4. The flash intensities (photons μm^{-2}) delivered on the step light for GCAPs$^{-/-}$ retina were 120 for first 5 traces, 500, and 1.6×10^3. The step light intensities in (A) and (B) are the same as in Fig. 5(A) and Fig. 5(B), respectively. (C) Fractional sensitivity (S_F/S_F^D) as a function of background intensity. Flash sensitivity (S_F) was determined by dividing the peak amplitude of dim flash response by the flash intensity and the maximal response amplitude for each retina. S_F^D is the flash sensitivity in darkness. Averages of control retinas (filled circles) and GCAPs$^{-/-}$ (open circles) retinas. Solid curves are best fitting Weber-Fechner functions with I_s = 12,900 (control) and 1,100 (GCAPs$^{-/-}$) photons μm^{-2} s^{-1}. The dotted curve represents the expected change in sensitivity of GCAPs$^{-/-}$ cones in the absence of adaptation (see Eqn. (4)). (D) Relative sensitivity (S_F/S_F^D) as a function of the residual amplitude ($R_{max}/R_{max, dark}$) for control and GCAPs$^{-/-}$ cones. Combined data from Fig. 5C and Fig. 6C. Residual amplitude determines the internal calcium concentration; as the residual amplitude declines, the internal calcium concentration becomes low. The decline in sensitivity against the reduction of calcium concentration was substantially shallower in GCAPs$^{-/-}$ retinas than in control retinas demonstrating the impaired cone adaptation in the absence of GCAPs. The parameters of the best fitting power functions (solid lines) are 2.94 for control cones and 2.35 for GCAPs$^{-/-}$ cones. The dotted line represents the expected change in sensitivity in the absence of Ca^{2+}-modulation (Eqn. (4)) in GCAPs$^{-/-}$ cones. Error bars show SEM.
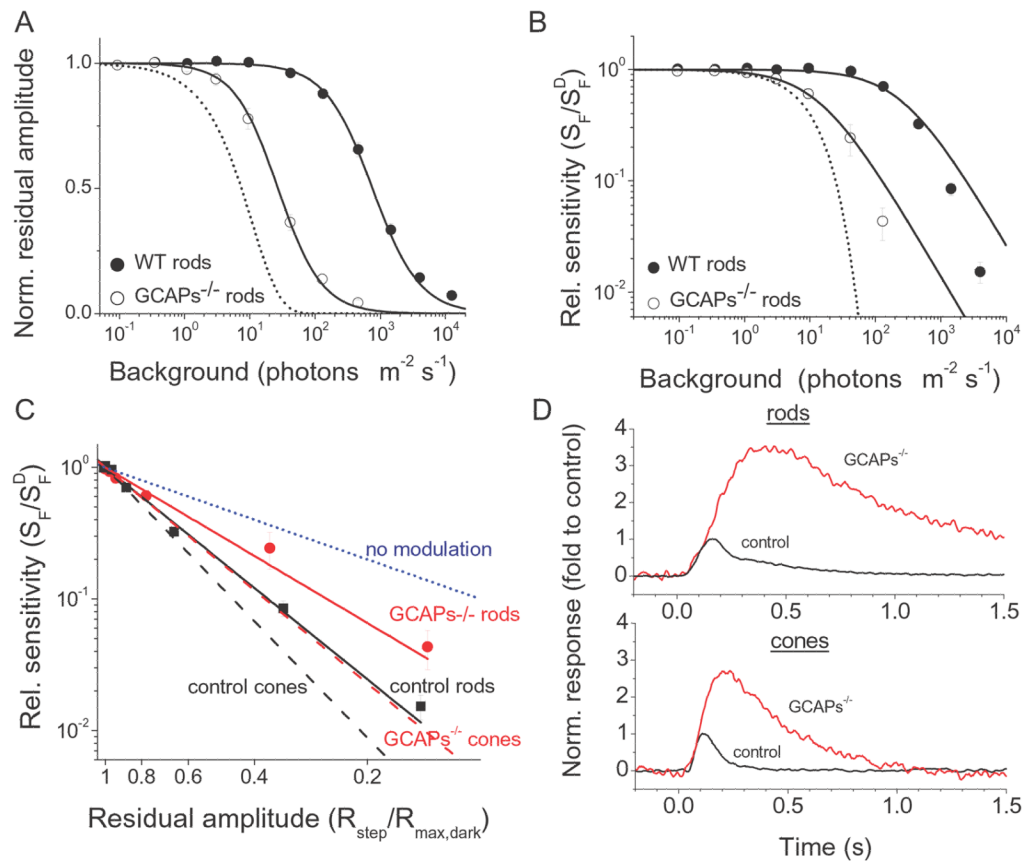
Figure 7.
(A) Normalized maximum rod responses as a function of background intensity for control (black circles, n = 10) and GCAPs$^{-/-}$ (open circles, n = 7) retina. The smooth curves represent best-fitted Hill equation with k = 1.20 and 1.29, I_R = 756 and 27 photons $\mu m^{-2} s^{-1}$ for control and GCAPs$^{-/-}$ rods, respectively. Error bars show SEM. The dotted curve represents the expected change in maximum response of GCAPs$^{-/-}$ rods in the absence of adaptation (Eqn. (4)). (B) Relative sensitivity as a function of background intensity. Flash sensitivity (S_F) was determined for each retina by dividing the peak amplitude of dim flash response by the flash intensity and the maximal amplitude for each retina. S_F^D is flash sensitivity in darkness. Averages of control (closed circles, n = 10) and GCAPs$^{-/-}$ (open circles, n = 7) retinas. Solid lines are best fitting Weber-Fechner functions with I_S = 272 (WT) and 14 (GCAPs$^{-/-}$) photons $\mu m^{-2} s^{-1}$. The dotted curve represents the expected change in sensitivity of GCAPs$^{-/-}$ rods in the absence of adaptation (Eqn. (4)). (C) Relative sensitivity (S_F/S_F^D) as a function of residual amplitude ($R_{max}/R_{max, dark}$). The decline in sensitivity against the reduction of residual amplitude (indicative of calcium level) for both rods and cones was substantially shallower in GCAPs$^{-/-}$ retinas than in control retinas. The parameters of the best fitting power functions are 2.30 for control rods (solid black line) and 1.69 for GCAPs$^{-/-}$ rods (solid red line). The dashed lines are the fitting functions for control cones (black) and GCAPs$^{-/-}$ cones (red) from Fig. 6D. The blue dotted line represents the expected change in sensitivity in the absence of Ca^{2+}-modulation. Error bars show SEM. (D) Single photon responses of rods (top) and cones (bottom) normalized by dividing them by their respective control peak amplitudes. The time of divergence of the GCAPs$^{-/-}$ (red) responses from control (black) responses was 120 ms for rods and 85 ms for cones.

Table 1

Parameters of cone suction recordings

	unit	control	control + BAPTA	GCAPs$^{-/-}$	GCAPs$^{-/-}$ + BAPTA
I$_o$	photons μm^{-2}	3415 ± 857 (12)	3035 ± 851 (10)	1248 ± 78 (16)	2390 ± 1173 (8)
R$_{max}$	pA	4.5 ± 0.7 (12)	4.2 ± 0.6 (10)	6.2 ± 0.8 (16)	7.7 ± 1.1 (8)
Time to peak	ms	112 ± 4 (12)	152 ± 17 (10)	221 ± 9 (16)	207 ± 24 (8)
Integration time	ms	112 ± 10 (12)	258 ± 67 (10)	374 ± 23 (16)	382 ± 36 (8)

Mean ± SEM (n). I$_O$ is the flash strength which generates half-maximal response.

Table 2

Parameters of cone ERG recordings

	unit	control cones	GCAPs$^{-/-}$ cones
I_o	photons μm^{-2}	2180 ± 380 (13)	918 ± 110 (13) [*]
R_{max}	μV	13.5 ± 0.6 (13)	16.2 ± 1.0 (13) [*]
Time to peak	ms	121 ± 4 (13)	211 ± 5 (13) [**]
Integration time	ms	183 ± 28 (13)	423 ± 21 (13) [**]
S_F^D	photons^{-1} μm^2	$3.7E\text{-}04 \pm 6.5E\text{-}05$ (13)	$1.0E\text{-}03 \pm 1.4E\text{-}04$ (13) [**]
I_S	photons μm^{-2} s^{-1}	12900 ± 3100 (7)	1100 ± 280 (7) [*]
I_R	photons μm^{-2} s^{-1}	94300 ± 26100 (7)	3900 ± 770 (7) [*]
k, Hill coefficient		0.47 ± 0.04 (7)	0.70 ± 0.03 (7) [**]

Mean $\pm$ SEM (n). Student's t-test determined significant differences

[*]
$p < 0.05$,

[**]
$p < 0.005$. IS is parameter of Weber-Fechner function in Fig. 6 C. I$_R$ and k are parameters obtained from the fit with eqn. (2) in Fig. 5C.

Table 3

Parameters of rod ERG recordings

	unit	control rods (n = 10)	GCAPs$^{-/-}$ rods (n = 7)
I_o	photons μm^{-2}	19 ± 3	11 ± 1
R_{max}	μV	89 ± 9	83 ± 9
Time to peak	ms	163 ± 5	389 ± 11
Integration time	ms	336 ± 33	1025 ± 39
$S_F{}^D$	photons^{-1} μm^2	2.6E-02 ± 3.1E-03	9.1E-02 ± 2.0E-02
I_S	photons μm^{-2} s^{-1}	272 ± 30	14 ± 3
I_R	photons μm^{-2} s^{-1}	756 ± 92	27 ± 10
k		1.20 ± 0.07	1.29 ± 0.20

Mean ± SEM. $S_F{}^D$ is a flash sensitivity in darkness. I_S is a background intensity, which gives half the flash sensitivity in Fig. 7 B. I_R and k are parameters obtained from the fit with eqn. (2) in Fig. 7A.